Relative Iris Codes

Peeranat Thoonsangngam, Somying Thainimit, Vutipong Areekul

***Abstract*—This paper proposes a new scheme to generate iris codes based on relative measure of local iris texture. The local characteristic of iris texture is analyzed using 2D Gabor wavelets. Twelve Gabor kernels, four frequencies and three orientations, are constructed and convoluted with an iris image. To inherit relationship of local iris texture among pixels, Gabor magnitude and phase of a reference pixel is compared with Gabor magnitudes and phases of the other four pixels. These pixels are located away from the reference pixel by $8\times d$ pixels, where d=1, 2, …, 4. Each comparison, a 2-bit primitive iris code is generated. Least significant bit of the primitive code describes how Gabor magnitudes of the two pixels are related. This bit is set to '1' if Gabor magnitude of a reference pixel is less than magnitude of the other pixel, otherwise it is set to '0'. Another bit of the 2-bit primitive code describes relative measure of the obtained phase values. This bit is set to '1' if difference of the obtained phases is within $\pm\pi/2$, otherwise it is set to '0'. In our scheme, each pixel is described using an 8-bit iris code. Matching between two iris codes is implemented using a look-up table technique. The table contains a number of matches of the primitive code of the two iris codes. By utilizing the look-up table technique, computational time of our 1:1 matching scheme is 2.2 milliseconds. Equal-Error-Rate (EER) of the proposed system using CASIA1.0 iris database is 0.0003%EER.**

***Index Terms*—Biometrics, iris texture analysis, iris recognition, relative iris codes.**

I. INTRODUCTION

DUE to demands of having higher and better security system for today society, an iris pattern recognition system becomes very attractive. As human iris patterns are highly distinctive, stable and hard to forge. Human iris patterns are formed during the first eighth month of gestation and remained the same structure after about one year old. Change of iris structure caused from diseases is rare. The structure is also stable across environments such as hot/cold etc. Human iris pattern is very unique. It is estimated that chance of having identical irises is 1 in 10^{78}[1]. An iris recognition system is a non-invasive recognition system, since appearance of iris patterns is visible at distance.

The idea of an automatic iris recognition system was firstly proposed by Flom and Safir [2] in 1987. But not until 1994, the first commercialized iris recognition system was introduced. The system algorithm was invented by Daugman [3]. Daugman generated a 1024-bit iris code using phase information obtained from a set of 2D Gabor wavelets. Matching of two iris codes was evaluated using hamming distance. Wildes [4] analyzed iris features using four-level Laplacian pyramid and Fisher classifier. Similarity measure of the obtained images was computed based on normalized correlation at various image scales. Boles et al [5] represented iris features using zero-crossing of multi-resolution 1D wavelet. His system was evaluated by finding dissimilarity value of the two iris templates at different scales. Ma et al [6, 7] extracted iris features using circular symmetric filters and multi-Gabor filters. They later developed an iris recognition system based on local intensity variations [8, 9]. Muron [10] and Miyazawa [11] analyzed iris textures using Fourier transform. Monro [12] extracted iris features using zero crossing of 1-D DCT. Several other works [13-19] have been proposed.

In this paper, we propose to encode human iris pattern using distribution of relative measure of local iris texture. The distribution of relative measure is significant information for personal identification task. Considering iris textures under circled areas of two different irises shown in Fig 1, these textures can be easily distinguished if relative distribution is considered. In addition, relative measure is less sensitive to noise.

The proposed method analyzes local characteristic of iris textures using 2D-Gabor Wavelets. A set of 2-D Gabor masks is constructed and convoluted with an iris image. The convolution generates two values: its magnitude and phase. The magnitude value indicates degree of characteristics matched between the mask and iris texture under the mask. Large magnitude is obtained when iris texture contains similar frequency and orientation characteristics as Gabor mask. Gabor phase value indicates phase information of the iris texture. Due to the two values convey significant and different characteristic of iris texture, both values are encoded into our iris code. Primitive element of our iris code is 2 bits long. One bit explains how magnitudes of two pixels are related, whereas another bit explains how their phases are related. Distribution of relative information of local iris texture is constructed by comparing relative measure of local iris textures at a distance. Features of one particular pixel are compared to features of other four pixels located further away.

The remainder of this paper is organized as follows: section II describes our proposed iris recognition, including iris localization, iris normalization and enhancement, iris feature extraction and encoding, and matching. Section III reports our experimental results. Section IV is our conclusions.

Manuscript received July 1, 2007. All Authors are with Kasetsart Signal and Image Processing Laboratory (KSIP Lab), Department of Electrical Engineering, Faculty of Engineering, Kasetsart University, Jatujak, Bangkok, 10900, Thailand. (e-mail: g4765155, fengsyt, fengvpa@ku,ac,th)

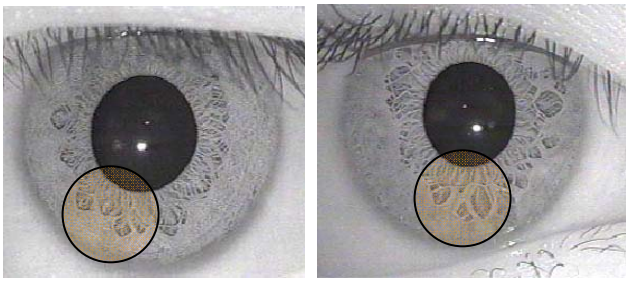

Fig. 1. Intensity distribution in two different irises.

II. Our Proposed Iris Recognition

Our iris recognition approach is composed of four main steps: 1) localization, 2) normalization and enhancement, 3) feature extraction and encoding, and 4) matching. Details are described as follows.

A. Iris Localization

Iris localization is to locate inner and outer boundaries of an iris. The inner boundary of an iris is a boundary separating the iris from the pupil. The outer boundary is a boundary separating the iris from the sclera. In our work, these two boundaries are modeled using two concentric circles.

Locating an iris inner boundary is to locate boundary of a pupil. Procedures of our pupil localization are shown in Fig 2. The first step of our scheme is smoothing an eye image with lowpass filter to reduce some noises. The second step is thresholding an image in order to separate regions of low intensity levels from the rest. The obtained regions often include pixels belong to pupil and eyelashes. The next step is finding edges using edge detection and edge thinning. Results of these operations often include edges of pupil, eyelashes and reflected lights. The obtained irrelevant edges are removed by examining its circularity and length of its diameter. Last step is fitting the obtained edges with a circular model. The fitting yields two parameters: r-inner and center coordinate of the pupil. This center is used as a reference point for the rest of the proposed approach.

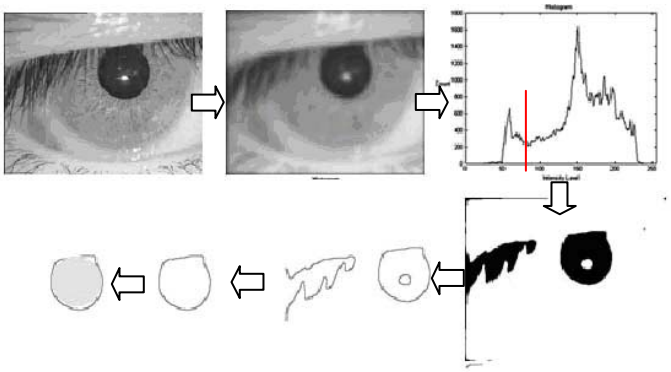

Fig. 2. A procedure of pupil localization

Fig.3. depicts steps to locate an iris outer boundary. The outer boundary of an iris is detected by searching for first abrupt change between iris and sclera. To make the search more accurate, contrast enhancement algorithm [20] is firstly applied to the image. This is to improve contrast nearby the boundary area. Differences of average intensity of pixels along circle arcs, as shown in Fig.3., having radius r_i and r_{i+1} are computed. The outer boundary is located where the obtained difference is over pre-specified threshold.

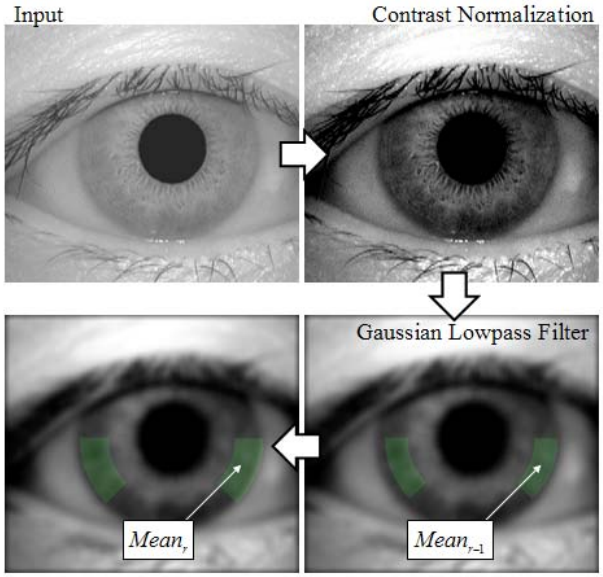

Fig. 3. A procedure of outer iris boundary localization.

B. Iris Normalization and Enhancement

Due to the contraction of the pupil responding to different amount of incoming light during capturing eye images, the segmented iris rings usually have different sizes. To compensate this variation, the segmented iris ring is normalized into one fixed size of rectangle using the following equation:

$$r_{input} = \{(i/N)\times(R_{outer} - R_{inner})\} + R_{inner},$$
$$\theta_{input} = (2\pi \times j)/M \qquad (1),$$

where, $(r_{input}, \theta_{input})$ is a polar coordinate of a point (x,y) of an input image, as shown in Fig.4(a). R_{inner} is an iris inner boundary. R_{outer} is an iris outer boundary. A point (i,j) is a corresponding point of $(r_{input}, \theta_{input})$ on the rectangle with a size of $N\times M$, as shown in Fig.4(b). This polar-rectangular mapping often causes misaligned $(r_{input}, \theta_{input})$ coordinates, which is solved by using bilinear interpolation.

Fig 5 shows examples of normalized iris images. Since a circular model is used, irrelevant objects such as portions of eyelids always include in a normalized image. To reduce noises caused from these irrelevant objects, only region nearby pupillary zone is used for the rest procedures.

After normalization, an iris image is enhanced using local histogram equalization. This operation aims to enhance iris texture and also to compensate non-uniform illumination distribution within an image. Fig 5 shows examples of the

enhanced iris image over the working region.

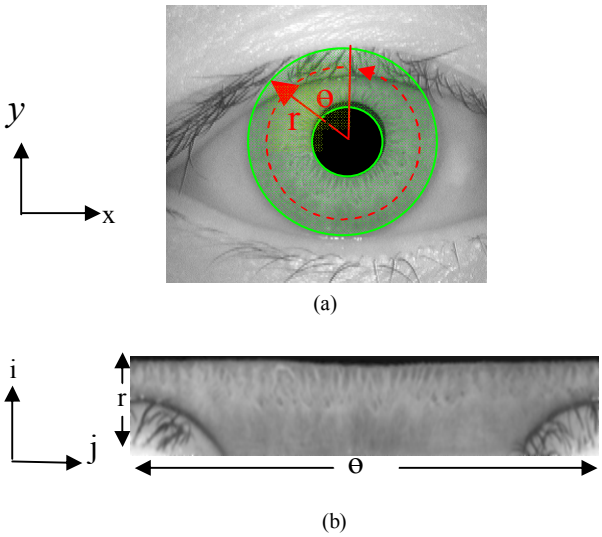

Fig 4. Iris normalization: (a) a polar coordinate of an input eye, (b) a rectangular coordinate of the normalized iris mage.

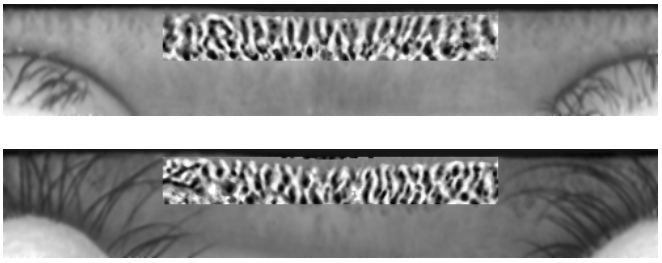

Fig.5. Examples of the enhanced iris images.

C. *Feature Extraction and Encoding*

After image enhancement, local characteristic of iris textures are analyzed and extracted using 2D Gabor wavelets. The Gabor wavelets are local spatial bandpass filters, that theoretically provide optimal conjoint resolution of information of a signal in 2D spatial and frequency domains [21]. As a result, Gabor wavelets are often used in texture analysis. Constructing Gabor filters is done by modulating sine and cosine carriers with a Gaussian. The cosine modulation yields real part Gabor component, whereas the sine modulation yields imaginary part. These two parts are often called even- and odd- symmetric Gabor component, respectively. Gabor function is defined as:

$$G(x,y) = Ke^{-\pi(a^2(x-x_0)^2+b^2(y-y_0)^2)}e^{-j2\pi(u_0(x-x_0)+v_0(y-y_0))}, \quad (1)$$

where (x_0,y_0) specifies spatial location of peak of the Gaussian envelop, (a,b) specifies the width of Gaussian envelop on x- and y- axis, and (u_0,v_0) specifies spatial frequency of the sinusoidal carriers. Orientation of Gabor filter is defined as $\theta = \tan^{-1}(v_0/u_0)$. In this work, all Gabor parameters are empirically selected to give the system the best Equal Error Rate (EER) tested using CASIA1.0 iris database [22]. Fig. 6 depicts a set of 12 Gabor kernels, 4 frequencies and 3 orientations, used in our work. Each kernel has a size of 35×16 pixels.

To analyze iris texture, the constructed kernels are horizontally convoluted with an enhanced iris image. Convolution of cosine kernel yields real value (*re*), whereas convolution of sine kernel yields imaginary value (*im*). Magnitude (M) and phase (ψ) of convoluting an image with Gabor kernel of size N are calculated as follows:

$$M = \frac{\sqrt{re^2 + im^2}}{N}, \qquad \psi = \arctan\left(\frac{im}{re}\right) \quad (2).$$

The obtained magnitude value indicates similarity level between characteristic of Gabor kernel and iris textures. Large magnitude value tells that iris texture is dominated by the same frequency and orientation of the tuned Gabor kernel. The obtained phase value reflects discontinuity in the phase of the iris texture.

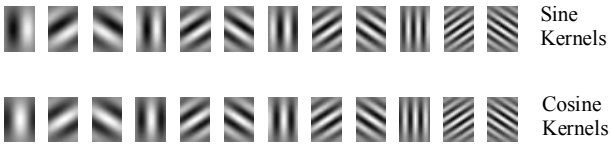

Fig. 6. The four frequencies and three directions of 2D Gabor kernels.

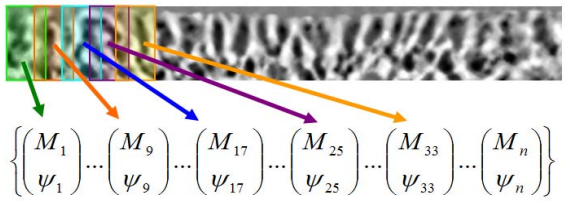

Fig.7. Five placements used in coding an 8-bit RMPB code.

Since both values carry different meanings, both values are used to construct an iris code. Instead of using the magnitude and phase information directly, relative information between a pixel and its surroundings is encoded. This is due to relative measure is less sensitive and more robust to noises. The relative information is obtained by comparing magnitude and phase value of a reference pixel, located at column '*i*', with magnitude and phase values obtained from other four pixels located at column $j = i+8\times d$, where d = 1, 2, ..., 4. The five placements of the Gabor masks are shown in Fig.7.

For each comparison, a 2-bit code is generated. One bit represents relative magnitude and another bit represents relative phase information. The least significant bit of the 2-bit code is set to '1' if magnitude of a reference pixel is less than magnitude of the other pixel. The most significant bit of

the 2-bit code is set to '1' if phase value of the reference pixel leads or lags phase value of the other pixel less than $\pi/2$. Table 1 indicates comparison conditions used in constructing the 2-bit code.

Considering one reference pixel, four comparisons are performed and an 8-bit iris code is constructed. This 8-bit code inherits information of how local iris texture is distributed around the reference pixel. Based on the size of our masks and an iris image, there are 205×12×8 = 2460-byte. Later on, we will call this code as 'relative magnitude and phase between blocks', or RMPB in short.

TABLE I
CONDITIONS FOR ENCODING A 2-BIT RMPB PRIMITIVE IRIS CODE

Magnitude	Phase	2-bit Code
$M_i \le M_j$	$\lvert\psi_i - \psi_j\rvert < \frac{\pi}{2}$ or $\lvert\psi_i - \psi_j\rvert > \frac{3\pi}{2}$	11
	$\frac{\pi}{2} \le \lvert\psi_i - \psi_j\rvert \le \frac{3\pi}{2}$	01
$M_i > M_j$	$\lvert\psi_i - \psi_j\rvert < \frac{\pi}{2}$ or $\lvert\psi_i - \psi_j\rvert > \frac{3\pi}{2}$	10
	$\frac{\pi}{2} \le \lvert\psi_i - \psi_j\rvert \le \frac{3\pi}{2}$	00

D. Matching

In our approach, similarity degree of two iris codes is determined using 2-bit hamming distance. The two 2-bit codes are considered as match if both bits of the two codes are the same. When a match of two 2-bit codes is found, a system matching score is incremented by one. Suppose we have an 8 bits long iris code, a matching score of comparing this code with itself is 4, not 8.

Benefit of designing the 2-bit code using a binary number is that calculating a matching score of two codes can be done using a looking up table technique. This technique is a fast technique.

In prior, a matching score table, size of 256×256, is created. The number of rows and columns of the table indicates the number of possibilities of the two codes we would like to find a match. To make a size of matching score compact, a length of codeword is 8 bits. The row index of the table associates to one 8-bit RMPB code (CW1), and column index of the table associates to another 8-bit RMPB code (CW2). A value contains inside the table cell indicates a number of match between these two codes. For example, a number of matches between two RMPB codes: '00000001' and '00001001' is 3. Therefore, looking up a matching score table at row '00000001' and column '00001001' retrieves a value of 3. Fig.8. shows a flowchart of our matching score table generation.

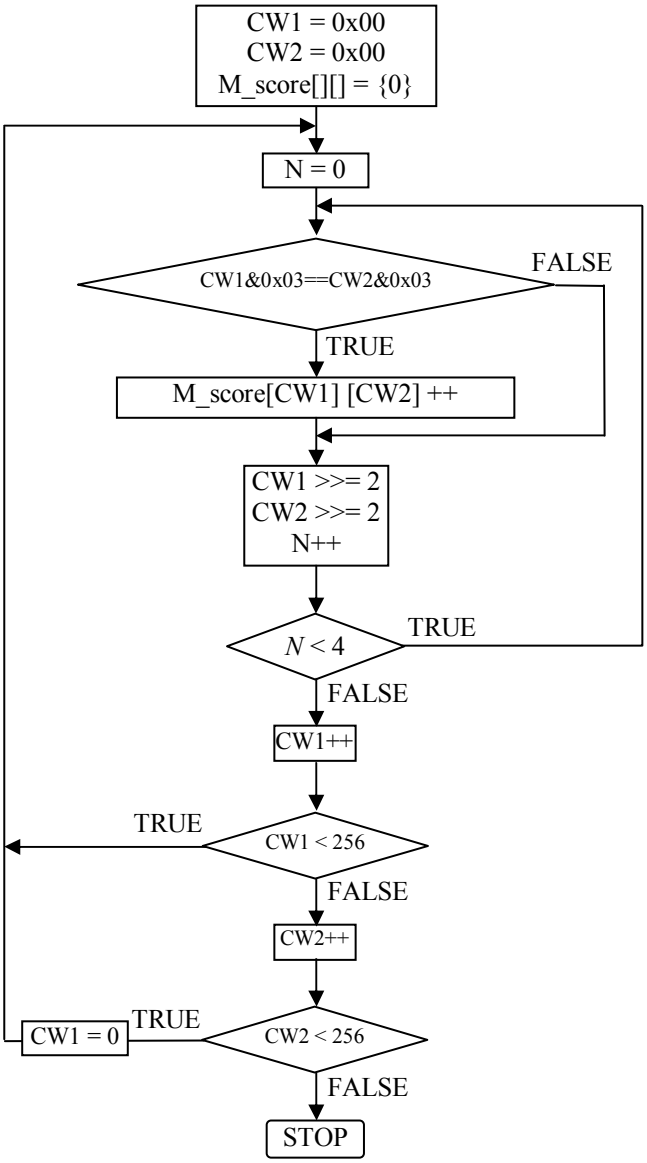

Fig.8. Flowchart of generating a matching score table

To compute total matching score of two iris codes, the matching score table is iteratively looking up. Since the length of our iris code is 2460 bytes, comparing two iris codes requires 2460 look-ups. This number of look-ups is multiplied by 21 to search for the best matching score of the system. The searching is to compensate rotation variance caused during acquisition process. Due to normalization process, rotation problem is translated to shifting an iris code. In our system, an iris code is shifted horizontally 21 times to find the matching scores. The best-obtained matching score is accounted for the system matching score. Total number of look-ups is, therefore, 2460×21 = 51,660 times.

III. EXPERIMENTAL RESULTS

We tested and evaluated our proposed iris recognition systems using two iris databases: CASIA1.0 and KSIP DB01R database. CASIA 1.0 database is a public database. It contains 756 iris images captured from 108 individual eyes. Each eye

has 7 images. This database is selected in order to compare our work with previous works. KSIP DB01R iris database is our own iris collection. The database contains 1920 iris images, captured from both eyes of 120 Thais volunteers, eight images for each eye. Fig. 9 shows examples of eye images of both databases. Major differences between the two databases are:

- Eyelash occlusions are often found in iris regions of the eyes of KSIP database.
- Shape of pupils of the eyes of KSIP database is closed to ellipse more than circle.
- Pupil region of eyes in KSIP is not prior filled with a black circle.

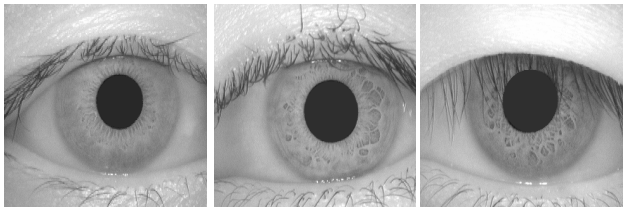

(a) CASIA1.0

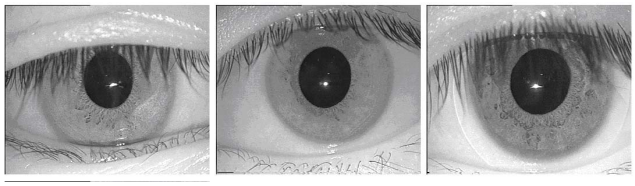

(b) KSIP DB01R

Fig. 9. Samples of eye images of (a) CASIA1.0 (b) KSIP DB01R.

To evaluate our system performance, each iris image is compared with the other images in the database. Fig. 10 shows the distribution of intra-class and inter-class matching distance of the two databases. For CASIA database, the distribution of the intra-class matching distance is estimated using $7c2 \times 108 = 2{,}268$ comparisons, and the distribution of the inter-class matching distance is estimated using $108c2 \times 7^2 = 283{,}112$ comparisons. Our experiments found no false for this database. This is due to size of the database is quite small. The Equal-Error-Rate (EER) of the system is thus estimated by statistically fitting the obtained data. The fitting gives a value of 0.0003%EER.

For KSIP database, the distribution of the intra-class matching distance is estimated with $8c2 \times 240 = 6{,}720$ comparisons and the distribution of the inter-class matching distance is estimated with $240c2 \times 8^2 = 1{,}835{,}520$ comparisons. Our experiments yield 0.383974%EER. It is clearly seen that results of CASIA database are outperformed results of KSIP. Major problems cause from irrelevant noises due to inaccurate iris localization. Since most pupils in KSIP database have an oval shape, modeling pupil using circle is inappropriate. Changing the model to Ellipsoid is our future work. In addition, KSIP database exhibits more eyelash noise than CASIA database. However, our proposed method provides better results comparing to existing systems. The comparison using CASIA1.0 database is shown in table II.

TABLE II.
SYSTEM PERFORMANCE COMPARISON OVER CASIA 1.0

Methods	EER (%)
Kazuyuki Miyazawa et al.[10]	0.00320
Peng Yao et al.**	0.28000
Chia-Te Chou et al. **	0.02290
Daugman*	0.00049
Tan*	0.00089
Monro*	0.00055
Proposed	0.00030

* see [11] for details, ** see [18] for details.

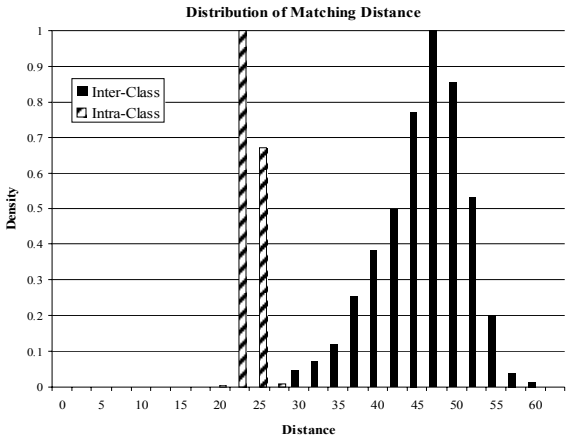

(a)

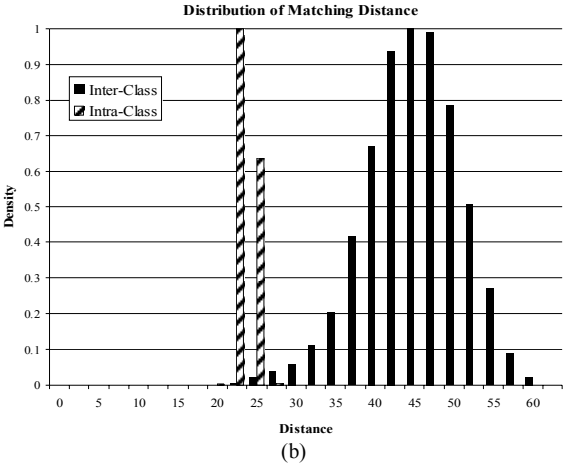

(b)

Fig.10. Intra- and Inter-class distribution distance of (a) CASIA1.0 (b) KSIP DB01R.

Due to table look-up technique, computational time of 1:1 matching is significantly reduced. Table III indicates computational time of the proposed algorithm. The algorithm is implemented using C++ on PC Pentium IV 2.4 GHz with 512 MB RAM.

TABLE III.
COMPUTATIONAL TIME OF THE PROPOSED SYSTEM

Process	Computational Time (milliseconds)
Localization	234
Normalization	31
Enhancement	212
Feature Extraction and Encoding	62
Matching (1:1)	2.2

IV. CONCLUSIONS

This paper proposes a new scheme of iris feature extraction and encoding for person authentication task. Major goal of the proposed scheme is to integrate distribution of relative information of local iris texture among neighbors into an iris code. Characteristic of local iris textures is analyzed and extracted using 2D Gabor wavelets. A set of Gabor masks with four frequencies and 3 orientations are constructed and convolved with an iris image. Local iris textures are then described using Gabor's parameters and values obtained from the Gabor masks. The descriptors are frequency, orientation, magnitude and phase values.

To encode an iris code, a primitive element is designed to have 2 bits long. One bit describes relative magnitude measures of two pixels, and another bit described relative phase measure of the two pixels. The magnitude bit is set to one if Gabor magnitude of a reference pixel is less than the other pixel, otherwise it is set to zero. The phase bit is set to one if the absolute difference phase values of the two pixels is less than $\pi/2$. Next, an 8 bits iris code is constructed based on the 2-bit code using one reference pixel and the other four pixels. The 8-bit code embeds distribution information of how local iris texture of reference pixel related to the other four pixels. These pixels are ones located away by distance of $8\times d$ pixels, where d = 1,2,..4. Inheriting relative information into an iris code makes our system less sensitive to noises.

Matching score of two iris codes is computed based on 2-bit hamming distance. The score is proportional to a number of matches of primitive elements of the two iris codes. We speed up our system computational time by using table look-up technique to compute matching score between two codes. A matching score table, containing a number of primitive matches between two 8-bit codes, are generated in prior. Matching score of two codes is, then, obtained by iteratively looking up this table at indices associated to the two codes.

Our proposed method has been evaluated using two databases: CASIA1.0 and KSIP DB01R. The Equal-Error-Rate (EER) of CASIA database is 0.0003%, whereas the EER of KSIP is 0.3839%. The second database gives worse system accuracy due to noises caused from occlusions and improper model of pupil. Our future works are toward implementing more accurate iris localization method.

REFERENCES

[1] J. Daugman and C. Downing, "Epigenetic Randomness, Complexity, and Singularity of Human Iris Patterns," Proc Rocal Soc. (London) B: Biological Science., vol. 268, pp. 1737-1740, 2001.

[2] L. Flom, A. Safir, "Iris Recognition System.," U.S. Patent No. 4, pp. 641 349, 1987

[3] J. Daugman, "High Confidence Visual Recognition of Persons by a Test of Statistical Independence," IEEE Trans. on PAMI., vol. 15, no.11, pp. 1148-1161, 1993.

[4] R.P. Wildes, J. Asmuth, G. Green, S. Hsu, R. Kolczynski, J. Matey, S. McBride, "A Machine-vision System for Iris Recognition.," Mach. Vis. Applic., vol. 9, pp.1-8, 1996.

[5] W.W. Boles, B.Boashah , "A Human Identification Technique using Images of the Iris and Wavelet Transform," IEEE Trans. on Signal Processing, vol..46, pp1185-1188, 1998.

[6] L. Ma, T. Tan, Y. Wang, "Iris Recognition Based on Multichannel Gabor Filters," Proceedings of the Fifth Asian Conference on Computer Vision, vol I, pp. 279-283, 2002.

[7] L. Ma, T. Tan, Y. Wang, D. Zhang, "Personal Identification Based on Iris Texture Analysis," IEEE Trans. on PAMI, vol. 25, no.12, pp. 1519-1533,2003.

[8] L. Ma, T. Tan, Y. Wang, D. Zhang, "Local Intensity Variation Analysis for Iris Recognition," Pattern Recognition, Vol. 34, pp. 1287-1298, 2004.

[9] L. Ma, T. Tan, Y. Wang, D. Zhang, "Efficient Iris Recognition by Characterizing Key Local Variations," IEEE Trans. on Image Processing, vol. 13, no. 6, pp. 739-750, 2004.

[10] Muron, P. Kors, J. Pospisil, "Identification of Person by Means of the Fourier Spectral of the Optical Transmission Binary Methods of Human Irises," Optics Communication, vol. 192, pp. 161-167, 2001.

[11] K.Miyazawa, K.Ito, T.Aoki, K.Kobayashi, H.Nakajima, "A Phase-Based Iris Recognition Algorithm," Proceedings of Int. Conf. on Biometrics (ICB), LNCS 3832, pp. 356-365, 2006.

[12] D.M. Monro, S. Rakshit, D. Zhang, "DCT-Based Iris Recognition," IEEE Trans. on PAMI, vol. 29, no.4, pp. 586-594, 2007.

[13] E. Krichen, M.A. Ellakh, S.Gracia-Salicetti, B. Dorizzi, "Iris Identification Using Wavelet Packets," Proceedings of 16th Int. Conf. on. Pattern Recognition (ICPR),, vol. 4, pp. 335-338, 2004.

[14] J. Cui, Y. Wang, L. Ma, T. Tan, Z. Sun, "An Iris Recognition Algorithm Using Local Extreme Points," Proceedings of Int. Conf. on Biometric Authentication (ICBA), LNCS 3072, pp.442-449, 2004.

[15] Zhenan Sun, Yunhong Wand, Tieniu Tan, and Jiali Cui, "Cascading Statistical and Structural Classifiers for Iris Recognition," Proceedings of Int. Conf. on Image Processing (ICIP), pp.1261-1264, 2004.

[16] C. Liu, M. Xe, "Iris Recognition Based on DLDA," Proceedings of 18th Int. Conf. on Pattern Recognition (ICPR), vol. 4, pp. 489-492, 2006.

[17] P. Yao, J. Li, X. Ye, Z. Zhuang, B. Li, " Iris Recognition Algorithm Using Modified Log-Gabor Filters," Proceedings of Int. Conf. on Pattern Recognition (ICPR) , vol. 4., pp. 461-464, 2006.

[18] Chia-Te Chou, Sheng-Wen Shih, Wen-Shiung Chen, Victor W. Cheng, "Iris Recognition with Multi-Scale Edge Type Matching," Proceedings of Int. Conf. on. Pattern Recognition (ICPR), vol 4, pp. 545-548, 2006.

[19] P. Thoonsaengngam, K. Horapong, S. Thainimit, and V. Areekul, "Efficient Iris Recognition using Adaptive Quotient Thresholding," Proceedings of Int. Conf. on Biometrics (ICB), LNCS 3832, pp. 472-478, 2006.

[20] L.Hong, Y.wan and A.K.Jain, "Fingerprint image enhancement: algorithm and performance evaluation," IEEE Trans. on PAMI, vol.20, no.8, pp.777-789, August 1998.

[21] Tai Sing Lee, "Image Representation using 2D Gabor Wavelets," IEEE Trans. on PAMI, vol. 18, no. 10, pp.959-971 October, 1996.

[22] http://nlpr-web.ia.ac.cn/english/irds/irisdatabase.htm